



Structure–activity relationships and molecular modeling of the *N*-(3-pivaloyloxy-2-benzylpropyl)-*N'*-[4-(methylsulfonylamino)benzyl] thiourea template for TRPV1 antagonism

Rahul S. Bhondwe^a, Dong Wook Kang^b, Myeong Seop Kim^a, Ho Shin Kim^a, Seul-gi Park^c, Karam Son^c, Sun Choi^c, Krystle A. Lang Kuhs^d, Vladimir A. Pavlyukovets^d, Larry V. Pearce^d, Peter M. Blumberg^d, Jeewoo Lee^{a,*}

^a Research Institute of Pharmaceutical Sciences, College of Pharmacy, Seoul National University, Seoul 151-742, Republic of Korea

^b Department of Pharmaceutical Science and Technology, College of Health and Medical Science, Catholic University of Deagu, Gyeongsan-si, Gyeongsangbuk-do 712-702, Republic of Korea

^c National Leading Research Lab (NLRL) of Molecular Modeling & Drug Design, College of Pharmacy, Division of Life & Pharmaceutical Sciences, and National Core Research Center for Cell Signaling & Drug Discovery Research, Ewha Womans University, Seoul 120-750, Republic of Korea

^d Laboratory of Cancer Biology and Genetics, Center for Cancer Research, National Cancer Institute, NIH, Bethesda, MD 20892, USA

ARTICLE INFO

Article history:

Received 20 March 2012

Revised 5 April 2012

Accepted 7 April 2012

Available online 13 April 2012

Keywords:

Vanilloid receptor 1

TRPV1 antagonist

Capsaicin

Resiniferatoxin

Molecular modeling

ABSTRACT

The structure–activity relationships of *N*-(3-acyloxy-2-benzylpropyl)-*N'*-4-[(methylsulfonylamino)benzyl] thioureas, which represent simplified RTX-based vanilloids, were investigated by varying the distances between the four principal pharmacophores and assessing binding and antagonistic activity on rTRPV1. The analysis indicated that a 3-pivaloyloxy-2-benzylpropyl C-region conferred the best potency in binding affinity and antagonism. The molecular modeling of this best template with the tetrameric homology model of rTRPV1 was performed to identify its binding interactions with the receptor.

© 2012 Elsevier Ltd. All rights reserved.

The transient receptor potential V1 (TRPV1) receptor¹ is a molecular integrator of nociceptive stimuli, including protons,² heat,³ inflammatory mediators such as anandamide⁴ and lipoxygenase products,⁵ and vanilloids such as capsaicin (CAP)⁶ and resiniferatoxin (RTX).⁷ The receptor functions as a non-selective cation channel with high Ca²⁺ permeability and its activation leads to an increase in intracellular Ca²⁺ that results in excitation of primary sensory neurons and ultimately the central perception of pain.

TRPV1 antagonists are promising drug candidates. Therapeutic applications include inhibiting the transmission of nociceptive signaling from the periphery to the CNS as well as blocking other pathological states associated with this receptor. TRPV1 antagonists have thus emerged as novel and promising analgesic and anti-inflammatory agents, particularly for chronic pain and inflammatory hyperalgesia.⁸ The number of antagonists reported continues to increase and their clinical development has been extensively reviewed.^{9–13}

Previously, we have reported that a series of *N*-(3-acyloxy-2-benzylpropyl)-*N'*-4-[(methylsulfonylamino)benzyl] thiourea analogues (e.g. **1** and **2**) were effective antagonists of the action of

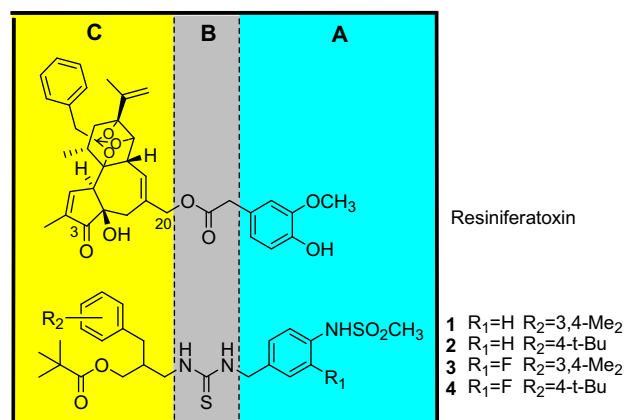


Figure 1. Pharmacophoric regions of RTX and sRTX.

* Corresponding author.

E-mail address: jeewoo@snu.ac.kr (J. Lee).

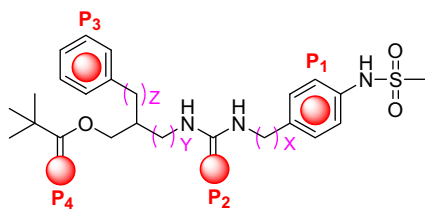


Figure 2. The four principal pharmacophores of sRTX.

capsaicin on rat TRPV1 (Fig. 1).^{14–16} We further found that 3-fluoro substitution on the 4-(methylsulfonylamino)phenyl group in the A-region enhanced the extent of antagonism.¹⁴ Thus, the compounds **3** and **4** showed high binding affinities and potent antagonism in the rat TRPV1/CHO system.

The principal pharmacophores in the template, denoted as P₁–P₄ in Figure 2, were derived from our RTX-derived pharmacophore model in which 4-hydroxy-3-methoxyphenyl (A-region), C₂₀-ester (B-region), orthophenyl (C₁-region) and C₃-keto (C₂-region) groups in RTX correspond to P₁–P₄, respectively.¹⁷

In order to find the optimal template and its active conformation for an sRTX (a simplified RTX having the four principal pharmacophores of RTX), we have investigated the structure–activity relationships of the template with regard to the spatial arrangement of key pharmacophores by lengthening or shortening the distances between the pharmacophores. We have already established from previous analysis that the distance between P₁ and P₂ was optimal when the linker is one-carbon (X = 1).¹⁵

In a continuation of these efforts, we have now optimized the distances between P₂ and P₄ in the template (corresponding to Y and Z in Fig. 2) with a (3-fluoro-4-methylsulfonylamino)benzyl A-region to obtain the preferred active spatial arrangement of four pharmacophores. We describe here the syntheses and functional TRPV1 activities of the designed ligands and our docking study of the resulting active template with our homology model.

General syntheses of the final target thioureas were achieved by the coupling between the corresponding isothiocyanates (or

thiocarbamate) and amines. For the template having Y = 0 and Z = 1, compounds **10** and **11** were synthesized by the coupling of the C-region amines **7** and **8** previously reported¹⁵ with the phenylthiocarbamate of A-region **9** (Scheme 1).

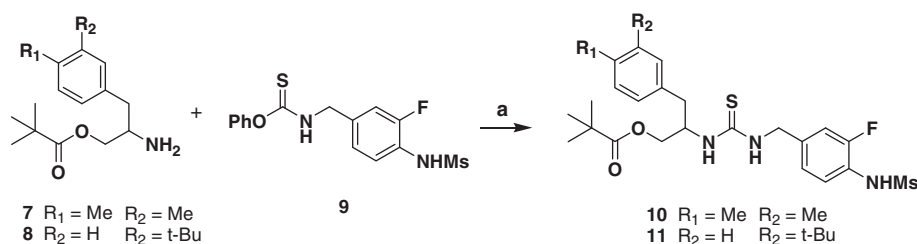
For the synthesis of a template having Y = 0 and Z = 2, the amines of the C-region **12** and **13** were prepared starting from *N*-(diphenylmethylene)glycine ethyl ester by the procedure reported previously¹⁵ and then were converted to the corresponding isothiocyanates, **14** and **15**. The isothiocyanates reacted with the amines of the A-region **16** and **17**¹⁴ to afford thioureas **18–21**, respectively (Scheme 2).

For the synthesis of a template having Y = 0 and Z = 0, the isothiocyanate of the C-region **25** was prepared starting from vinylbenzene **22** in four steps (Scheme 3). The dihydroxylation of **22** followed by selective pivaloylation provided **23** whose hydroxyl group was converted to the corresponding azide **24**. The azide **24** was then converted to the isothiocyanate **25** efficiently with carbon disulfide and triphenylphosphine.¹⁸ The isothiocyanate **25** was coupled with the amines of the A-region **16** and **17** to afford the final compounds **26** and **27**.

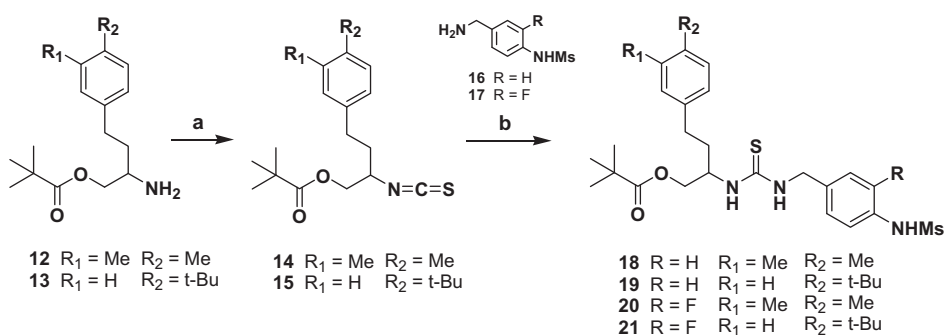
For the synthesis of a template having Y = 1 and Z = 0, the isothiocyanate of the C-region **31** was prepared starting from 2-phenylacetate **28** in five steps (Scheme 4). The C-acylation of **28**, the reduction of the diester followed by selective pivaloylation provided alcohol **29**. By following the route represented in Scheme 3, compound **29** was converted to the final thioureas **32** and **33**.

The binding affinities and potencies as agonists/antagonists of the synthesized TRPV1 ligands were assessed in vitro by a binding competition assay with [³H]RTX and by a functional ⁴⁵Ca²⁺ uptake assay using rat TRPV1 heterologously expressed in Chinese hamster ovary (CHO) cells, as previously described.¹⁹ The results are summarized in Table 1, together with the potencies of the previously reported thiourea antagonists **1–6**.^{14–16}

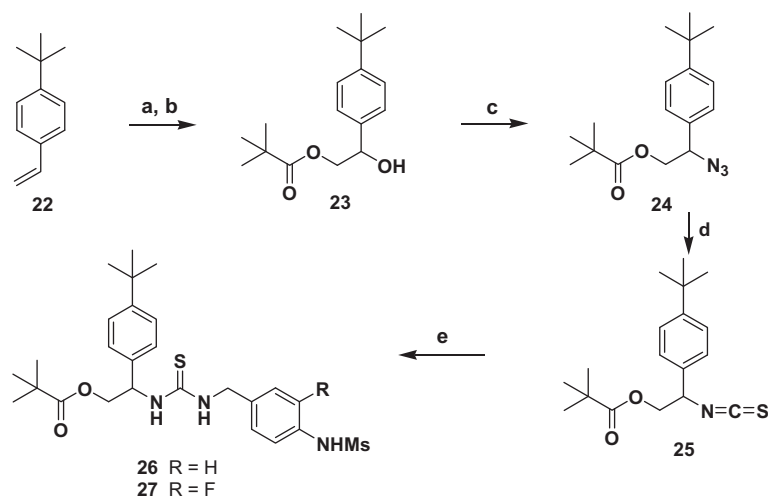
Previously, the analysis of the SAR for the spacing between P₁ ((4-methylsulfonylamino)phenyl) and P₂ (thiourea) (the A and B-regions, respectively) indicated that either one-carbon elongation or one-carbon deletion between them caused a dramatic loss of binding affinity regardless of the distances between P₂ and P₄.



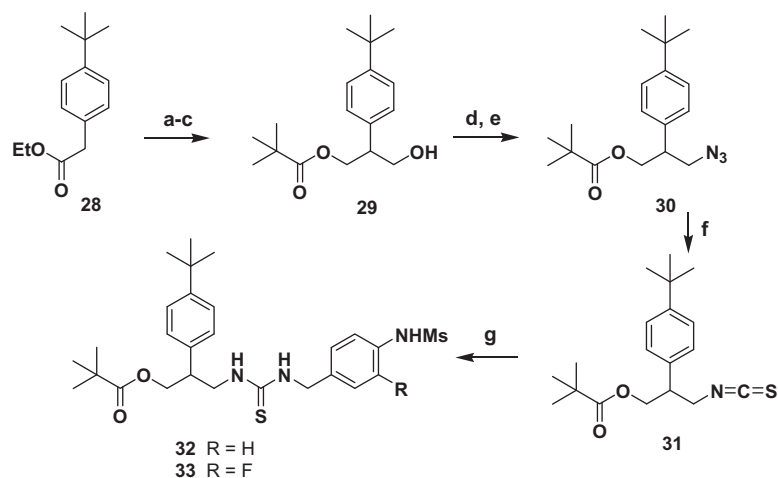
Scheme 1. Reactions and conditions: (a) NEt₃, CH₂Cl₂, 90–95%.



Scheme 2. Reactions and conditions: (a) 1,1'-thiocarbonyl diimidazole, NEt₃, DMF, 80–85%; (b) NEt₃, CH₂Cl₂, 90–95%.



Scheme 3. Reactions and conditions: (a) OsO₄, NMO, acetone–H₂O (1:1), 84%; (b) pivaloyl chloride, NEt₃, DMAP, CH₂Cl₂, 95%; (c) DPPA, DBU, toluene, 65%; (d) CS₂, PPh₃, THF, 74%; (e) **16** or **17**, NEt₃, CH₂Cl₂, 90–95%.



Scheme 4. Reactions and conditions: (a) NaOEt, diethyl carbonate, toluene, 58%; (b) LiAlH₄, ether, 85%; (c) pivaloyl chloride, NEt₃, DMAP, CH₂Cl₂, 95%; (d) MsCl, NEt₃, CH₂Cl₂, 92%; (e) NaN₃, DMF, 82%; (f) CS₂, PPh₃, THF, 78%; (g) **16** or **17**, NEt₃, CH₂Cl₂, 90–95%.

Thereby, the SAR in the present study was conducted based on the template of the *N*-[(4-methylsulfonylamino)benzyl]thiourea template corresponding to *X* = 1 in Figure 2.

In the variation of the *Y* part of the template, one-carbon shortening of **1** and **2** (*Y* = 1, *Z* = 1) provided *N*-(2-pivaloyl-1-benzylethyl) analogues **5** and **6** (*Y* = 0, *Z* = 1), which were found to be partial antagonists with weaker binding affinities by 20- and 6.5-fold, respectively. Modification of the *A*-region through incorporation of a fluoro group into **5** and **6** at the 3-position in the *A*-region led not only to stronger binding affinities (2.5-fold for **10**, 3.6-fold for **11**) but also to enhanced antagonism, as we would predict from previous studies.¹⁴

In the variation of the *Z* part of the template, one-carbon shortening of **2** and **4** (*Y* = 1, *Z* = 1) provided *N*-(3-pivaloxy-2-phenylpropyl) analogues **32** and **33** (*Y* = 1, *Z* = 0), which were found to be full antagonists despite a modest loss in binding affinities of 2.2- and 3-fold, respectively.

The combination of one-carbon shortening of the *Y* part and one-carbon elongation of the *Z* part of analogues **1–4** (*Y* = 1, *Z* = 1) provided *N*-[2-pivaloyl-1-(phenylethyl)ethyl] analogues **18–21** (*Y* = 0, *Z* = 2), which exhibited reduced potencies in binding affinity and variable effects on antagonistic potencies. The

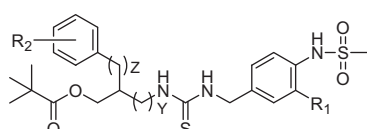
extremes were a 2-fold enhancement in antagonistic potency for **18** compared to **1** and a 14-fold reduction in potency for **20** compared to **3**. On the other hand, one-carbon shortening of both the *Y* and *Z* parts from **2** and **4** (*Y* = 1, *Z* = 1) afforded *N*-(2-pivaloyl-1-phenylethyl) analogues **26** and **27** (*Y* = 0, *Z* = 0), which also showed weaker binding affinities but became partial agonists/antagonists in contrast to the above template.

Overall, the SAR analysis of *Y* and *Z* parts in the *C*-region provided the order of potencies in their binding affinities as follows: (*Y*, *Z*) = (1, 1) > (1, 0) > (0, 0 ≈ 0, 1 ≈ 0, 2). We conclude that the *C*-region having *Y* = 1, *Z* = 1 together with *X* = 1 for the *A*-region provided the optimal sRTX for interacting with the rTRPV1.

We previously constructed the tetramer homology model of rat TRPV1 (rTRPV1) and reported the docking results of representative TRPV1 ligands, including capsaicin, resiniferatoxin (RTX) and sRTX.²⁰ Using this rTRPV1 model, we performed a flexible docking study with compound **4**, which possesses the highest binding affinity in this series.²¹ As shown in Figure 3, this molecule fitted well into the binding site located at the interface of the two monomers. The 4-(methylsulfonylamino) phenyl group (*A*-region) occupied the deep bottom hole at the binding site, and the two oxygen atoms and NH of the sulfonamide group participated in hydrogen

Table 1

Potencies of vanilloid ligands for binding to rat TRPV1 and for inducing calcium influx in CHO/TRPV1 cells



	Y	Z	R ₁	R ²	Binding affinity K _i ^a (nM)		Agonism ^b (%)	Antagonism K _i ^c (nM) (%)	
1	1	1	H	3,4-Me ₂	29.3	(±7.6)	(15)	67	(±25)
2	1	1	H	4- <i>t</i> -Bu	64	(±21)	(40)	86	(±17)
3	1	1	F	3,4-Me ₂	54	(±28)	NE	7.8	(±3.0)
4	1	1	F	4- <i>t</i> -Bu	22.6	(±2.7)	(5)	52	(±17)
5	0	1	H	3,4-Me ₂	580	(±130)	(19)		(48)
6	0	1	H	4- <i>t</i> -Bu	416	(±44)	(8)		(31)
10	0	1	F	3,4-Me ₂	233	(±18)	NE	650	(±210)
11	0	1	F	4- <i>t</i> -Bu	115	(±2.7)	NE	179	(±20)
32	1	0	H	4- <i>t</i> -Bu	143	(±43)	NE	91	(±25)
33	1	0	F	4- <i>t</i> -Bu	69	(±18)	NE	116	(±40)
18	0	2	H	3,4-Me ₂	390	(±100)	(5)	33.7	(±2)
19	0	2	H	4- <i>t</i> -Bu	366	(±8.1)	NE	286	(±48)
20	0	2	F	3,4-Me ₂	120	(±4.6)	NE	111	(±43)
21	0	2	F	4- <i>t</i> -Bu	190	(±38)	NE	152	(±46)
26	0	0	H	4- <i>t</i> -Bu	197	(±56)	(46)	940	(±420) (46)
27	0	0	F	4- <i>t</i> -Bu	244	(±46)	(35)	213	(±18) (72)

NE: not effective, WE: weakly effective at 30 μM.

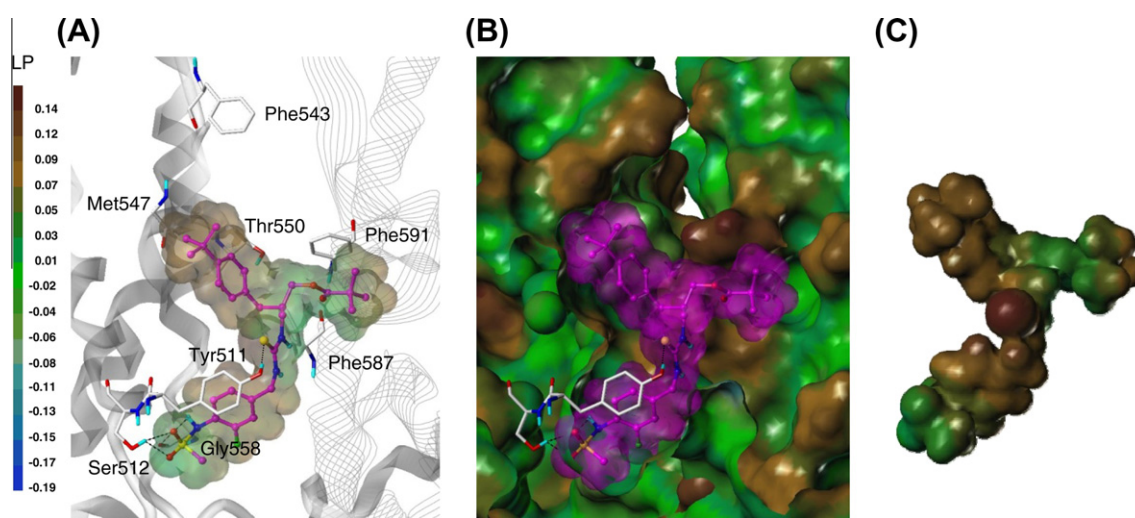
^a Mean ± SEM of at least three experiments.^b If any agonism was detected, value in parentheses indicates fractional calcium uptake compared to that by 30 μM capsaicin.^c Mean ± SEM of at least three experiments for measuring K_i. Value in parenthesis indicates measured extent of partial antagonism if observed.

Figure 3. Predicted binding mode of compound **4** in the rTRPV1 model with surface representations. (A) Binding mode of compound **4**. The key residues are marked and displayed as capped-stick with carbon atoms in white. The helices are colored in gray and the helices of the adjacent monomer are displayed in line ribbon. Compound **4** is depicted as ball-and-stick with carbon atoms in magenta. The van der Waals surface of the ligand is presented with the lipophilic potential property. Hydrogen bonds are shown in black dashed lines, and non-polar hydrogens are undisplayed for clarity. (B) Surface representations of the docked compound **4** and rTRPV1. The Fast Connolly surface of rTRPV1 was generated by MOLCAD and colored by the lipophilic potential property. The surface of rTRPV1 is Z-clipped, and that of the ligand is in its carbon color for clarity. (C) Van der Waals surface of compound **4** is colored by the lipophilic potential property.

bonding with Ser512 and Gly558, respectively. The sulfur of the thiourea group (B-region) made a hydrogen bond with Tyr511 and also contributed to the appropriate positioning of the C-region for the hydrophobic interactions. The bulky and hydrophobic 4-*t*-butylbenzyl and pivaloyloxymethyl groups in the C-region extended toward Met547 in the upper hydrophobic area and the adjacent monomer's hydrophobic region, composed of Phe587 and Phe591, and formed hydrophobic interactions.

In summary, we have investigated the structure–activity relationship of a series of *N*-(3-acyloxy-2-benzylpropyl)-*N'*-4-[(methylsulfonylamino)benzyl] thioureas as TRPV1 antagonists in which we varied the distances between the four principal pharmacophores (P₁–P₄). The analysis indicated that the C-region template having X = 1, Y = 1, and Z = 1 in Figure 2 displayed the best potency

in binding affinity and antagonism for rTRPV1, reflecting that its pharmacophores provided the optimal spacing for rTRPV1 interaction. The docking study of compound **4** with the tetrameric homology model established by us provided useful information on the binding interactions with the receptor, including the hydrophilic interactions with Tyr511 and Ser512 and the hydrophobic ones with the two separate pockets composed of Met547 and Phe587/591, respectively.

Acknowledgments

This research was supported by Grants from the National Research Foundation of Korea (NRF) (R11-2007-107-02001-0), Grants from the NLRL program (2011-0028885), Brain Research Center of

the 21st Century Frontier Research Program (2011-K000289) funded by MEST and NRF, the Ewha Global Top 5 Grant 2011 of Ewha Womans University, and was supported in part by the Intramural Research Program of the National Institutes of Health, Center for Cancer Research, National Cancer Institute (Project Z1A BC 005270).

References and notes

1. Szallasi, A.; Blumberg, P. M. *Pharmacol. Rev.* **1999**, *51*, 159.
2. Tominaga, M.; Caterina, M. J.; Malmberg, A. B.; Rosen, T. A.; Gilbert, H.; Skinner, K.; Raumann, B. E.; Basbaum, A. I.; Julius, D. *Neuron* **1998**, *21*, 531.
3. Caterina, M. J.; Schumacher, M. A.; Tominaga, M.; Rosen, T. A.; Levine, J. D.; Julius, D. *Nature* **1997**, *389*, 816.
4. Zygmunt, P. M.; Petersson, J.; Andersson, D. A.; Chuang, H.-H.; Sorgard, M.; Di Marzo, V.; Julius, D.; Hogestatt, E. D. *Nature* **1999**, *400*, 452.
5. Hwang, S. W.; Cho, H.; Kwak, J.; Lee, S. Y.; Kang, C. J.; Jung, J.; Cho, S.; Min, K. H.; Suh, Y. G.; Kim, D.; Oh, U. *Proc. Natl. Acad. Sci. U.S.A.* **2000**, *97*, 6155.
6. Walpole, C. S. J.; Wrigglesworth, R. *Capsaicin in the Study of Pain*; Academic Press, 1993. 63.
7. Appendino, G.; Szallasi, A. *Life Sci.* **1997**, *60*, 681.
8. Szallasi, A.; Cruz, F.; Geppetti, P. *Trends Mol. Med.* **2006**, *12*, 545.
9. Voight, E. A.; Kort, M. E. *Expert Opin. Ther. Pat.* **2010**, *20*, 1.
10. Lazar, J.; Gharat, L.; Khairathkar-Joshi, N.; Blumberg, P. M.; Szallasi, A. *Expert Opin. Drug Discov.* **2009**, *4*, 159.
11. Gunthorpe, M. J.; Chizh, B. A. *Drug Discovery Today* **2009**, *14*, 56.
12. Wong, G. Y.; Gavva, N. R. *Brain Res. Rev.* **2009**, *60*, 267.
13. Kym, P. R.; Kort, M. E.; Hutchins, C. W. *Biochem. Pharmacol.* **2009**, *78*, 211.
14. Lee, J.; Lee, J.; Kang, M.; Shin, M.-Y.; Kim, J.-M.; Kang, S.-U.; Lim, J.-O.; Choi, H.-K.; Suh, Y.-G.; Park, H.-G.; Oh, U.; Kim, H.-D.; Park, Y.-H.; Ha, H.-J.; Kim, Y.-H.; Toth, A.; Wang, Y.; Tran, R.; Pearce, L. V.; Lundberg, D. J.; Blumberg, P. M. *J. Med. Chem.* **2003**, *46*, 3116.
15. Lee, J.; Kim, S. Y.; Lee, J.; Kang, M.; Kil, M.-J.; Choi, H.-K.; Jin, M.-K.; Wang, Y.; Toth, A.; Pearce, L. V.; Lundberg, D. J.; Tran, R.; Blumberg, P. M. *Bioorg. Med. Chem.* **2004**, *12*, 3411.
16. Ryu, H.; Jin, M.-K.; Kang, S.-U.; Kim, S. Y.; Kang, D. W.; Lee, J.; Pearce, L. V.; Pavlyukovets, V. A.; Morgan, M. A.; Tran, R.; Toth, A.; Lundberg, D. J.; Blumberg, P. M. *J. Med. Chem.* **2008**, *51*, 57.
17. Lee, J.; Lee, J.; Kim, J.; Kim, S. Y.; Chun, M. W.; Cho, H.; Hwang, S. W.; Oh, U.; Park, Y. H.; Marquez, V. E.; Beheshti, M.; Szabo, T.; Blumberg, P. M. *Bioorg. Med. Chem.* **2001**, *9*, 19.
18. Isoda, T.; Hayashi, K.; Tamai, S.; Kumagai, T.; Nagao, Y. *Chem. Pharm. Bull.* **2006**, *54*, 1616.
19. Min, K. H.; Suh, Y.-G.; Park, M.-K.; Park, H.-G.; Park, Y.-H.; Kim, H.-D.; Oh, U.; Blumberg, P. M.; Lee, J. [published erratum appears in *Mol. Pharmacol.* **2003**, *63*, 958] *Mol. Pharm.* **2002**, *62*, 947.
20. Lee, J. H.; Lee, Y.; Ryu, H.; Kang, D. W.; Lee, J.; Lazar, J.; Pearce, L. V.; Pavlyukovets, V. A.; Blumberg, P. M.; Choi, S. *J. Comput. Aided Mol. Des.* **2011**, *25*, 317.
21. The docking study was conducted with the active (R)-isomer of compound **4**. The syntheses and biological characterization of chiral isomers will be published elsewhere. The 3D structure of the ligand was generated with concord and energy minimized using the MMFF94s force field and MMFF94 charge until the rms of the Powell gradient was 0.05 kcal mol⁻¹ Å⁻¹ in SYBYL-X 1.2 (Tripos Int., St. Louis, MO, USA). The flexible docking study on the rTRPV1 model²⁰ was performed by GOLD v. 5.0.1 (Cambridge Crystallographic Data Centre, Cambridge, UK), which uses a genetic algorithm (GA) and allows for full ligand flexibility and partial protein flexibility. The binding site was defined as 8 Å around the capsaicin docked in the rTRPV1 model. The side chains of the seven residues which are important for ligand binding (i.e., Tyr511, Ser512, Leu515, Phe543, Leu547, Thr550, and Asn551) were set to be flexible with 'crystal mode' in GOLD. The ligand was docked using the GoldScore scoring function with 30 GA runs. Other parameters were set as default. All computation calculations were undertaken on an Intel® Xeon™ Quad-core 2.5 GHz workstation with Linux Cent OS release 5.5.